AMPK-SIRT1-PGC1α Signal Pathway Influences the Cognitive Function of Aged Rats in Sevoflurane-Induced Anesthesia

Xiao-Yu Yang [1] · Qiu-Jun Li [1] · Wen-Chao Zhang [1] · Shao-Qiang Zheng [1] · Zhi-Jun Qu [1] · Yang Xi [1] · Geng Wang [1]

Abstract

To understand the effect of AMP-activated protein kinase (AMPK)-SIRT1 (silent information regulator 1)-PPARγ coactivator-1α (PGC1α) signaling pathway on the cognitive function of sevoflurane-anesthetized aged rats. Aged rats were divided into Normal group, Sevo group (Sevoflurane anesthesia), Sevo + AICAR (the AMPK activator) group, Sevo + EX527 group (the AMPK inhibitor), and Sevo + AICAR + EX527 group. The cognitive function of rats was determined by the Morris water maze. Hippocampal neuronal apoptosis was evaluated by TUNEL and Fluoro-Jade C (FJC) staining, and the expression of cleaved caspase-3 was detected by immunohistochemistry. ROS, SOD, and MDA levels and the fluorescence intensity of GFAP in the hippocampus were assayed. The mitochondrial membrane potential (MMP), mitochondrial mass, ATP level, and the expression of AMPK-SIRT1-PGC1α were determined by the corresponding methods. Rats in the Sevo group manifested significant extension in the escape latency, with fewer platform crossings; and meanwhile, the apoptotic rate, the number of FJC-positive cells, and the fluorescence intensity of GFAP of neurons were elevated, with up-regulation of cleaved caspase-3. Moreover, the level of MDA and ROS was increased evidently, with significant down-regulation of SOD activity, ATP, mitochondrial mass and MMP levels, and AMPK, SIRT1 and PGC-1α protein expressions. However, sevoflurane-induced changes above were improved after the administration of AICAR, and EX527 could reverse AICAR-induced improvements in Sevo-anesthetized aged rats. Activating AMPK-SIRT1-PGC1α pathway can improve the cognitive function and mitigate the neuronal injury in Sevo-anesthetized aged rats by antagonizing the oxidative stress and maintaining the mitochondrial function.

Keywords AMPK · SIRT1 · PGC1α · Sevoflurane · Cognitive function

Introduction

Postoperative cognitive dysfunction (POCD) refers to the decline in the mental activity, personality, social activity, and cognitive function, as compared with the baseline before operation (Li et al. 2017; Steinmetz et al. 2009). Clinically, the deterioration was mainly appeared in the memory, attention, and linguistic comprehension, as well as the alteration of social ability (Nesaratnam et al. 2014). Generally, POCD could not only decrease the life quality of patients but also pose severe burdens on the family and society (Liu and Han 2015). Various factors have been shown to involve in the cognitive dysfunction, while the inhalation of anesthetics may be considered as the major one (Davis et al. 2014; Jungwirth et al. 2009). For example, sevoflurane has been frequently applied in clinical anesthesia with the characteristics of a low blood-gas partition coefficient, rapid recovery, and minor stimulation to the airway (Delgado-Herrera et al. 2001). But the latest evidence pointed out the side effects of sevoflurane, which may induce POCD in elder patients by promoting the oligomerization of β-amyloid peptide (Aβ) and formation of fibrosum (Cremer et al. 2011; Hu et al. 2014). Also, sevoflurane can alter the cognitive function of rats by triggering inflammation, oxidative stress, and the imbalance of intracellular calcium homeostasis in the central nerve system, while the mechanism remains unknown (Haseneder et al. 2009; Zhang et al. 2013). Thus, it is significant to elucidate the pathogenesis of sevoflurane-induced POCD, thus improving the clinical anesthesia and surgical management.

AMPK, a highly conservative serine/threonine protein kinase, is critical to the regulation of homeostasis of cellular energy and the maintenance of neuronal morphology and function (Claret et al. 2007). SIRT1, as a member of the Sirtuins family, is able to antagonize the aging process, elongate the life span, and regulate the metabolism, which acts as

---

✉ Geng Wang
wangcheng_wc2514@163.com

[1] Department of Anesthesiology, Beijing Jishuitan Hospital, Beijing 100035, China

the major regulator for the biological development of mitochondria (Chung et al. 2010; Hwang et al. 2013). PGC1α is a member of the PGC1 family that is responsible for regulating the energy metabolism of brain and involved in a variety of neurodegenerative diseases (Austin and St-Pierre 2012). Evidence derived from the metabolism-related studies has shown that activated AMPK can increase the activity of AMPK-SIRT1-PGC1α pathway (Canto and Auwerx 2009). It was also reported that AMPK-SIRT1-PGC1α can sustain the balance in energy metabolism in the brain via modulating the mitochondrial function, thereby protecting the brain neurons (Chau et al. 2010). Dong et al. (2016) reported that $A\beta_{25-35}$ can suppress the signal transduction in AMPK/SIRT1-PPARγ-PGC1α axis, resulting in the mitochondrial injury, and anomaly in energy metabolism of brain, thereby developing the Alzheimer's disease. Furthermore, Cao et al. (2014) found that AMPK activation can improve the prenatal stress-induced cognitive dysfunction by regulating the mitochondrial function and oxidative stress. However, the role of AMPK-SIRT1-PGC1αpathway in sevoflurane-induced cognitive dysfunction remains unknown yet.

Thus, in this study, we explored the effect of AMPK-SIRT1-PGC1α pathway on the cognitive function of sevoflurane-anesthetized elder rats, aiming to provide a novel theoretical evidence for prophylaxis and treatment of sevoflurane-induced POCD.

Materials and Methods

Experimental Animals

Sixty clean healthy aged Wistar male rats (age, 19–20 months; weight, 600–650 g) were provided from the Shanghai Center of Laboratory Animals of Chinese Academy of Sciences. All rats were housed in a quiet, well-ventilated, clean animal room at regular day/night rhythm, with free access to the water and food, where the temperature was maintained between 21 and 23 °C, with the relative humidity of $60\% \pm 5\%$. The animal experiment was designed with the approval of the Ethical Committee of the Beijing Jishuitan Hospital, and all animal-involved procedures were conducted following the *Guidelines of the Use and Management of Laboratory Animals* published by National Institute of Health (Mason and Matthews 2012).

Model Establishment and Animal Grouping

All animals were divided into 5 groups with 12 rats in each group, including Normal group, Sevo group (rats anesthetized by sevoflurane), Sevo + AICAR group (sevoflurane-anesthetized rats received the intracerebroventricular injection of 50 μg AICAR, the activator of AMPK) (Du et al. 2015), Sevo + EX527 group (sevoflurane-anesthetized

rats received the intracerebroventricular injection of 30 μg EX527, the inhibitor of SIRT1) (Yan et al. 2013), and Sevo + AICAR + EX527 group (sevoflurane-anesthetized rats received the intracerebroventricular co-injection of EX527 and AICAR). Rats in the Normal group inhaled the air containing about 30% O_2, while rats in other groups inhaled the 2% sevoflurane following the intracerebroventricular injection. Inhalation would last for 5 h (Tian et al. 2015). Following 24 h, rats were subjected to the test of Morris water maze and then decapitalized to obtain the hippocampus that was incised into two parts, one being preserved at −80 °C and the other being fixed in 4% paraformaldehyde.

Morris water maze

Cognitive function was evaluated by the ZH0065 Morris water maze for 5 days, consisting of 4 days of negation test and 1 day of probe test, and all tests were started at 9:00 a.m. when water temperature maintained at 23 °C. Rats were placed into the water facing the wall and were allowed to swim freely in the maze for 120 s. The escape latency was counted from the time of entry to the time when rats found out the platform. Afterward, rats were allowed to stay on the platform for 30 s, and if rats failed to locate the platform within 120 s, they were guided to the platform and allowed to stay for 30 s. At the fifth day, the platform hidden under the water was evacuated, and rats were placed into the water to swim for 120 s, during which the number of crossings and stay duration in the target quadrant were recorded.

Terminal Deoxynucleotidyl Transferase-Mediated dUTP Nick-End Labeling (TUNEL) Assay

Hippocampus was fixed in 4% paraformaldehyde and then subjected to the regular treatment: dehydration in ethanol of gradient concentrations, clearing in xylene and embedding in paraffin. Thereafter, hippocampus tissues were sliced into the sections in thickness of 4 μm. Tissue sections were then used to perform the TUNEL staining as per the instructions of kit (Boehringer Mannheim), and the results were observed under the microscope. The apoptotic rate of neurons in hippocampus was calculated by the percentage of TUNEL-positive cells in all cells in CA1 region of hippocampus.

Fluoro-Jade C (FJC) Staining

FJC staining (Merck Millipore, Germany) was performed according to the operation instructions and used to detect degenerating neurons. In brief, the frozen sections were prepared, fixed, and immersed in a basic alcohol solution, consisting of 1% sodium hydroxide in 80% ethanol for 5 min, and then incubated in 0.06% potassium permanganate solution for 10 min. Following a 1–2 min water rinse, the slices were transferred for 10 min to a 0.0001% solution of

FJC dissolved in 0.1% acetic acid vehicle and then rinsed through three changes of distilled water for 1 min per change. The slices were air-dried, coverslips were applied, and the sections were visualized on an Image J software (Image J 1.4, NIH, USA). The data were presented by the average number of FJC-positive neurons in the fields.

Immunofluorescence Staining

Sections were blocked and permeabilized in 5% normal donkey serum with 0.3% Triton-X 100 in PBS for 2 h. Next, the slices were incubated with anti-GFAP (1:100, Carpinteria, CA) in a dark place overnight at 4 °C. The following day, the slices were thoroughly washed with PBS and incubated with the corresponding secondary antibodies for 1 h. Sections were mounted on slides and coverslipped with VECTASHIELD Mounting Media (Vector Labs), and images were taken with a Nikon C1 scanning confocal microscope (Nikon, Tokyo, Japan).

Immunohistochemistry

The hydrated paraffin tissue sections were subjected to the following treatment: antigen retrieval by citrate sodium, blocking the endogenous peroxidase for 10 min in peroxide hydrogen. Then, tissue sections were incubated with the rabbit anti-mouse cleaved caspase-3 polyclonal antibody (Cell Signaling Technology, USA) at 4 °C overnight and then incubated with the horseradish peroxidase (HRP)-conjugated secondary antibody for 10 min. The immunoblots were developed in diaminobenzidine (DAB) working solution, and the nucleus was counterstained in the hematoxylin. Thereafter, sections were mounted in neutral balsam and placed under the microscope to observe the results. The quantitative analysis was carried out using the Image Pro-Plus version 6.0 (IPP6, Media Cybernetics Inc., MD, USA) software to determine the positive signal using average integrated optical density (IOD) of the hippocampal CA1 section.

Measurement of Reactive Oxygen Species (ROS)

Hippocampus was placed in the icy normal saline for tissue homogenization in the ultrasound wave, and the resultant homogenate was then centrifuged at 1000 g and 4 °C to obtain the supernatant. In the supernatant, 10 μM of dichloro-dihydro-fluorescein diacetate (DCFH-DA) was added for incubation at 37 °C for 60 min without light, and the DCFH-DA was discarded. Remaining cells were rinsed in the serum-free medium for three times and collected by centrifugation. Cells were then re-suspended in 100 μL of phosphate buffer solution (PBS) to determine the fluorescence signals at 485/535 nm.

Measurement of MDA and SOD in Rat Hippocampus

Tissues were homogenized in the icy normal saline by the ultrasound wave and then subjected to the centrifugation at 1000 g and 4 °C to obtain the supernatant, followed by the measurement of malondial-dehyde (MDA) and superoxide dismutase (SOD) in hippocampus as per the instructions of kit (Boster, Wuhan, China).

Measurement of Mitochondrial Membrane Potential (MMP)

Hippocampus was dissected from rats to prepare the single-cell suspension, where the mitochondrial membrane potential-specific fluorescent probe JC-1 was added to label the mitochondria by incubating at 37 °C for 15 min (Beyotime, Shanghai, China). JC-1 was then removed by rinsing in PBS, and cell suspension was subjected to the measurement of mitochondrial membrane potential by using the flow cytometer (Becton Dickinson, USA).

Adenosine Triphosphate (ATP) Measurement

ATP measurement was carried out by luciferin-luciferase method using the ENLITEN® ATP Bioluminescence Detection kit (Promega, USA) in the following steps: Hippocampus tissues were homogenized in a homogenizer, and the resultant homogenate was then subjected to the centrifugation to obtain the supernatant at 1000 g and 4 °C. After the measurement of protein concentration by using the Bradford method, 50 μL samples were then added into each well to mix with 100 μL working solution of ATP detection, immediately followed by the measurement of relative luciferase unit (RLU) value by the Luminometer. The concentration of ATP in each sample was then calculated according to the standard curve.

Mitochondrial Mass Measurement

Mitochondrial mass was measured by using MitoTracker Green FM staining. Cells were stained with 400 nM MitoTracker Green FM (Invitrogen, Carlsbad, CA, USA) in minimum essential medium without serum for 30 min. MitoTracker Green FM-stained cells were quantified with a FACScan (Becton Dickinson, USA).

Western Blotting

Hippocampus was dissected from rats to prepare the cell lysate, where the total protein was extracted. According to the concentration of protein in each sample determined by the bicinchoninic acid (BCA) method, the protein in each sample was adjusted to the same concentration, and in each lane,

50 µg of protein sample was loaded to perform the electrophoresis in 10% SDS-PAGE. The separated proteins were then transferred on the PVDF membrane, where the unoccupied sites were blocked in 5% non-fat milk for 1 h at room temperature. Then, proteins on the membrane were incubated at 4 °C overnight with the following primary rabbit anti-mouse monoclonal antibodies: AMPK (ab80039, Abcam), SIRT1 (ab110304, Abcam), PGC-1α (ab106814, Abcam), and β-actin (ab8226, Abcam). Afterward, HRP-conjugated secondary antibodies (1:1000, Boster, Wuhan, China) were then added on the membrane to for further incubation with the immunoblots at room temperature for 1 h on a shaker. On the membrane, the resultant immunoblots were developed by incubating with the enhanced chemiluminescence (ECL) reagent (Pierce, USA). The relative protein content was expressed by the ratio of the intensity of target protein to that of β-actin.

Statistical Analysis

All data were subjected to the data analysis in SPSS 21.0 software. Measurement data were presented in form of mean ± standard deviation (SD) and compared among groups by one-way ANOVA followed by Turkey's post hoc test. Two-way ANOVA with factors treatment (different group) and session (time), the latter being repeated measures factor, was used for analysis of escape latency in the Morris water maze. Tukey's honestly significant difference test was used for post hoc testing. $P < 0.05$ represented the statistical significance of difference.

Results

Variation in Cognitive Functions of Rats in Each Group

The Morris water maze (Fig. 1) showed that in comparison with the rats in the Normal group, rats in the Sevo group manifested the significant extension in the escape latency but reduction in the platform crossings (all $P < 0.05$). However, as compared with the Sevo group, rats in the Sevo + AICAR group had significantly shortened escape latency and increase in the platform crossings, while those in the Sevo + EX527 group showed the opposite changes (all $P < 0.05$). In addition, in comparison with the rats in the Sevo + AICAR group, the escape latency of rats in the Sevo + AICAR + EX527 was extended significantly, with an obvious decrease in the platform crossings (all $P < 0.05$).

Neuronal Apoptosis and Degeneration in the Hippocampus of Rats

TUNEL staining and immunohistochemistry of cleaved caspase-3 (Fig. 2a–b) indicated that in comparison with the
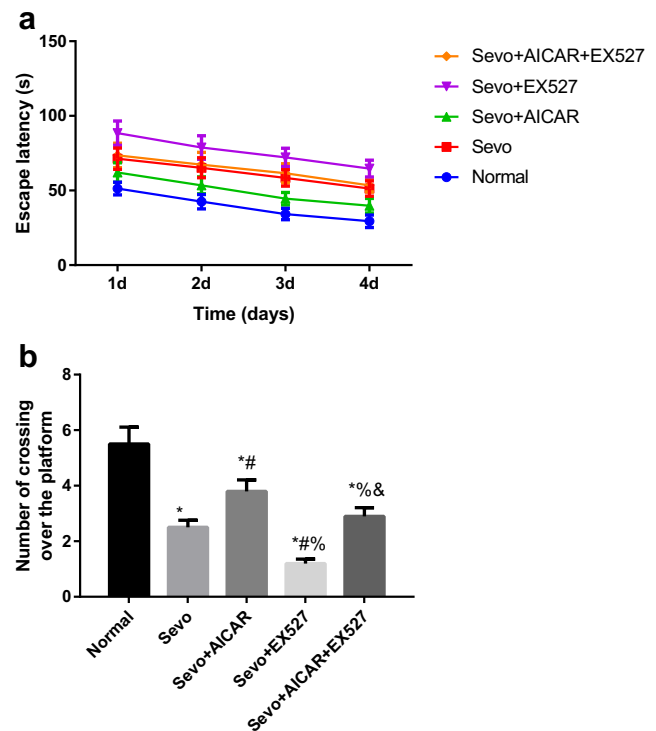

Fig. 1 Comparison of the alterations in the behavioral indicators of rats evaluated by Morris water maze. **a** Comparison of the escape latency of rats among groups; the quantitative data are the mean ± SD (two-way ANOVA followed by Turkey's post hoc test, $n = 12$). **b** Comparison of the number of platform crossings of rats among groups; the data are presented as the mean ± SD (one-way ANOVA followed by Turkey's post hoc test, $n = 12$). * $P < 0.05$ vs. the Normal group; # $P < 0.05$ vs. the Sevo group; % $P < 0.05$ vs. the Sevo + AICAR group; & $P < 0.05$ vs. the Sevo + EX527 group

Normal group, rats in the Sevo group had higher cell apoptotic rate and enhanced expression of cleaved caspase-3 in the CA1 region of hippocampus (all $P < 0.05$). As compared with the Sevo group, the apoptotic rate of neurons in CA1 region of hippocampus was decreased, with down-regulation of cleaved caspase-3 in the Sevo + AICAR group, while the EX527 resulted in the opposite changes (all $P < 0.05$). Furthermore, in comparison with the Sevo + AICAR group, co-treatment of AICAR + EX527 caused significant increases in the neuronal apoptosis and cleaved caspase-3 expression in CA1 region of rat hippocampus (all $P < 0.05$). As shown in Fig. 2c–d, the number of FJC-positive cells and the fluorescence intensity of GFAP were markedly increased in the Sevo + AICAR group compared with the Normal group (all $P < 0.05$). In addition, the number of FJC-positive cells and the fluorescence intensity of GFAP notably declined in the Sevo + AICAR group relative to the Sevo group, whereas they increased in the Sevo + EX527 group (all $P < 0.05$). In addition, the number of FJC-positive cells and the fluorescence intensity of GFAP increased in the Sevo + AICAR + EX527 group compared with the Sevo + AICAR group (all $P < 0.05$, Fig. 2g–h).
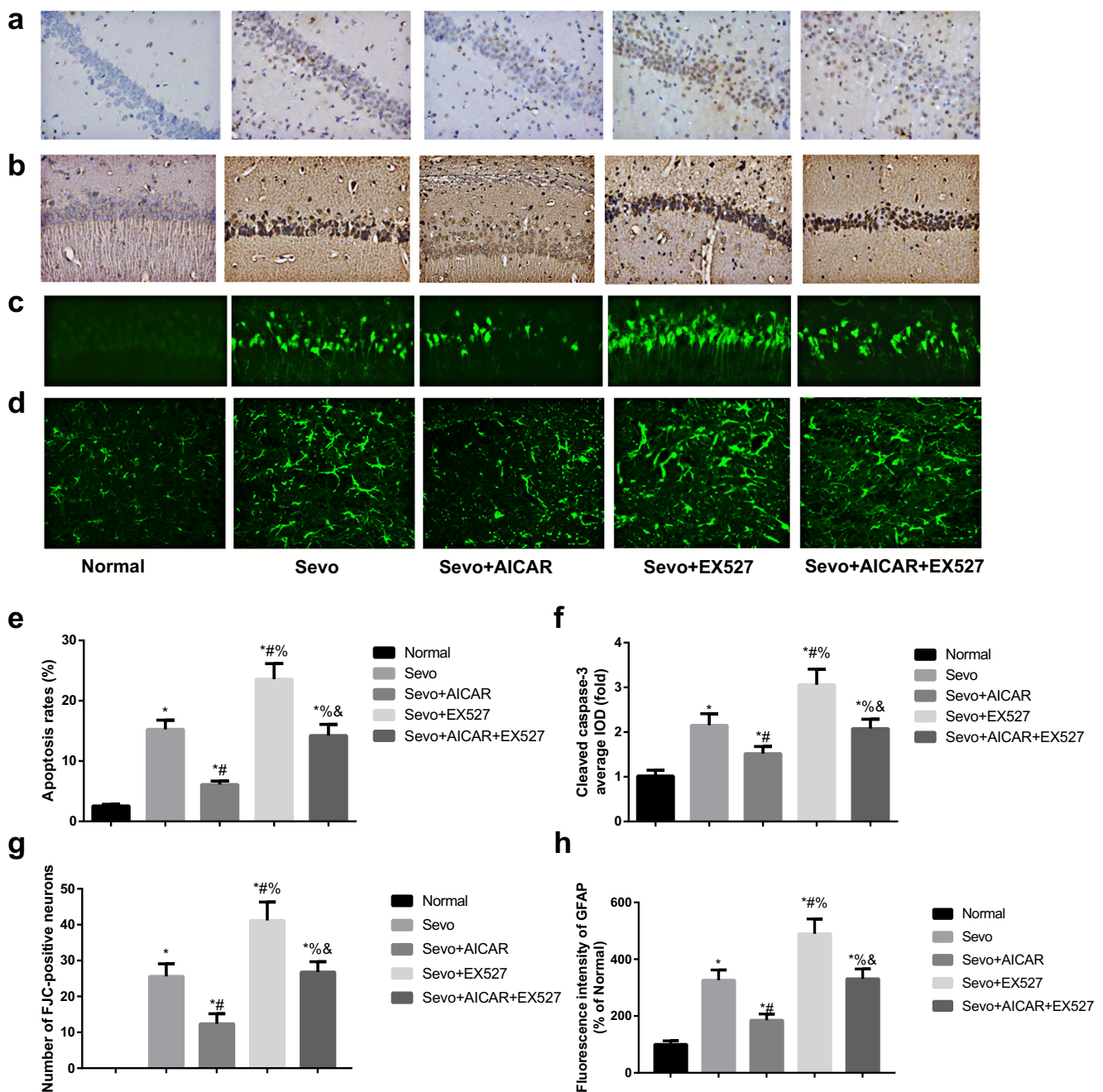
Fig. 2 Cell apoptosis in the CA1 region of rat hippocampus. **a** Cell apoptosis in CA1 region of rat hippocampus detected by TUNEL staining; **b** expression of cleaved caspase-3 in CA1 region of rat hippocampus detected by immunohistochemistry; **c** representative images of Fluoro-Jade C (FJC)-positive staining in CA1 region of rat hippocampus; **d** representative immunofluorescence staining images of GFAP, a marker of astrogliosis in CA1 region of rat hippocampus; comparison of the apoptotic rate of neurons (**e**), the average IODs of cleaved caspase-3 (**f**), the number of FJC-positive cells (**g**), and fluorescence intensity of GFAP (**h**) in CA1 region of rat hippocampus; the data are presented as the mean $\pm$ SD (one-way ANOVA followed by Turkey's post hoc test, $n = 12$). * $P < 0.05$ vs. the Normal group; # $P < 0.05$ vs. the Sevo group; % $P < 0.05$ vs. the Sevo + AICAR group; & $P < 0.05$ vs. the Sevo + EX527 group

Comparison of the Oxidative Stress of Rats

By comparison with the Normal group, MDA level in the rats of Sevo group was increased evidently, with a decrease in SOD activity and an increase in the relative generation of ROS (all $P < 0.05$, Fig. 3). In comparison with the Sevo group, MDA level was decreased evidently in the Sevo + AICAR group, while SOD activity was increased, and relative generation of ROS was decreased significantly; however, EX527 caused the opposite changes in rats of the Sevo + EX527 group ($P < 0.05$). Moreover, in comparison with the Sevo + AICAR group, co-treatment of AICAR and EX527
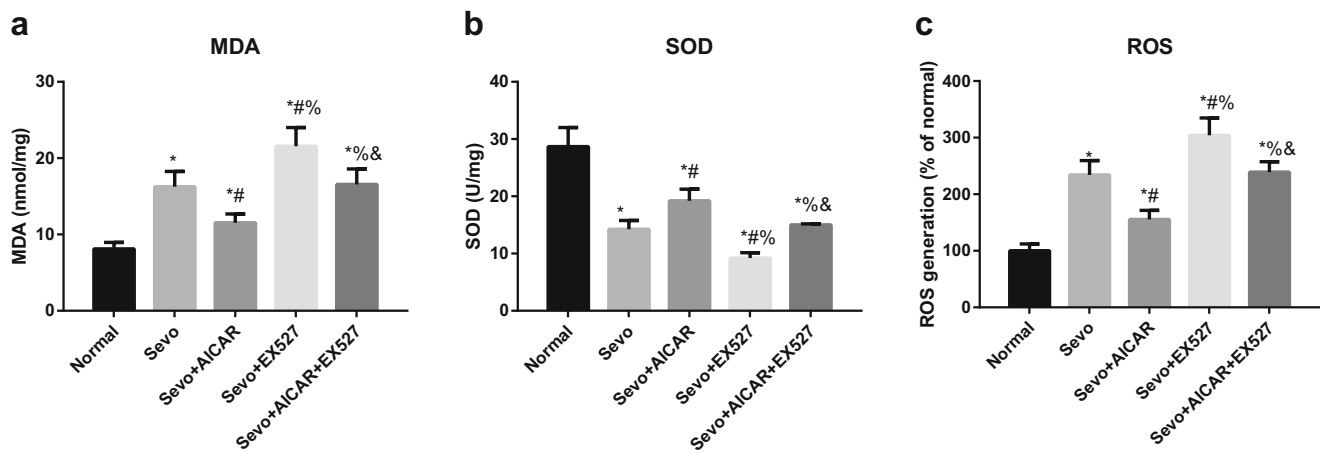
Fig. 3 Comparison of the oxidative stress of rats among groups. **a–c** Comparison of the MDA level, SOD activity, and relative generation of ROS in rats among groups; the quantitative data are the mean ± SD (one-way ANOVA followed by Turkey's post hoc test, $n = 12$). * $P < 0.05$ vs. the Normal group; # $P < 0.05$ vs. the Sevo group; % $P < 0.05$ vs. the Sevo + AICAR group; & $P < 0.05$ vs. the Sevo + EX527 group

contributed to the increase in the MDA level, decrease in SOD activity, and increase in the relative generation of ROS (all $P < 0.05$).

Comparison of Mitochondrial Membrane Potential (MMP), Mitochondrial Mass, and ATP Levels of Rats

As compared with the Normal group, the levels of ATP and MMP of rats in the Sevo group were decreased significantly (all $P < 0.05$). Mitochondrial mass, assessed by mean fluorescence intensity (MFI) of MitoTracker FM Green, was also significantly decreased in the Sevo + AICAR group compared with the Normal group ($P < 0.05$). Treatment of AICAR resulted in the higher levels of ATP, mitochondrial mass, and MMP in sevoflurane-induced rats, but on the contrary, the treatment of EX527 caused the converse changes (all $P < 0.05$). In addition, in comparison with the Sevo + AICAR group, ATP, mitochondrial mass and MMP levels were decreased in the Sevo + AICAR + EX527 group (all $P < 0.05$, Fig. 4).

Expression of AMPK-SIRT1-PGC-1α Pathway in Rat Hippocampus

Western blotting was carried out to determine the protein expression in the AMPK-SIRT1-PGC-1α pathway, and the results (Fig. 5) showed that in comparison with the Normal group, AMPK, SIRT1, and PGC-1α expressions were down-regulated significantly in the Sevo group (all $P < 0.05$). When comparing to the Sevo group, rats had significant up-regulations in AMPK, SIRT1, and PGC-1α in hippocampus of rats from the Sevo + AICAR group (all $P < 0.05$), whereas the AMPK expression between Sevo + AICAR group and Sevo + AICAR + EX527 group showed no significant difference ($P > 0.05$).

Discussion

Morris water maze is the regular behavioral test reflecting the learning and memory abilities, where the escape latency can indicate the learning ability, while the platform crossings suggest the memory function (Ning et al. 2017). The experimental elder rats in our study anesthetized by sevoflurane presented the prolonged escape, with an evident reduction in platform crossings (Gong et al. 2012; Liu et al. 2016), which was in line with the previous findings. Moreover, AICAR (the activator of AMPK) treated in elder rats led to the shortened escape latency and the increased platform crossings, while the treatment of EX527 (the inhibitor of SIRT1) resulted in the quite opposite changes. Likewise, Lu et al. (2010) reported that AMPK activation can decrease the Aβ generation and deposition in the brain of high-cholesterol-fed elder rats, thereby exerting the neuro-protective effect. Overexpression of AMPKα1, as reported by Yan et al. (Yan et al. 2019), can shorten the escape latency and prolong the stay in the target quadrant by up-regulating p-AMPK and SIRT1, thus improving the cognitive function. Kim et al. (2007) also found that the activation of SIRT1 can promote the neuron survival and reduce the nerve degeneration in hippocampus, ultimately blocking the learning disorder in the inducible p25 transgenic mouse. Also, the memory loss was alleviated in high-fat-diet-induced POCD elder rats in the work of Zhao et al. (2019) via activating SIRT1/PGC-1α expression. Especially, AICAR was demonstrated to increase the expressions of AMPK, SIRT1, and PGC-1α in our sevoflurane-anesthetized rats, while these changes are reversed by the treatment of EX527, with the deterioration in the cognitive function. According to the existing evidence, AMPK can induce the activation of SIRT1 by increasing the levels of nicotinamide adenine dinucleotide (NADH) (Chung et al. 2010; Xie et al. 2013), and the acetylation of SIRT1 can further activate or promote the
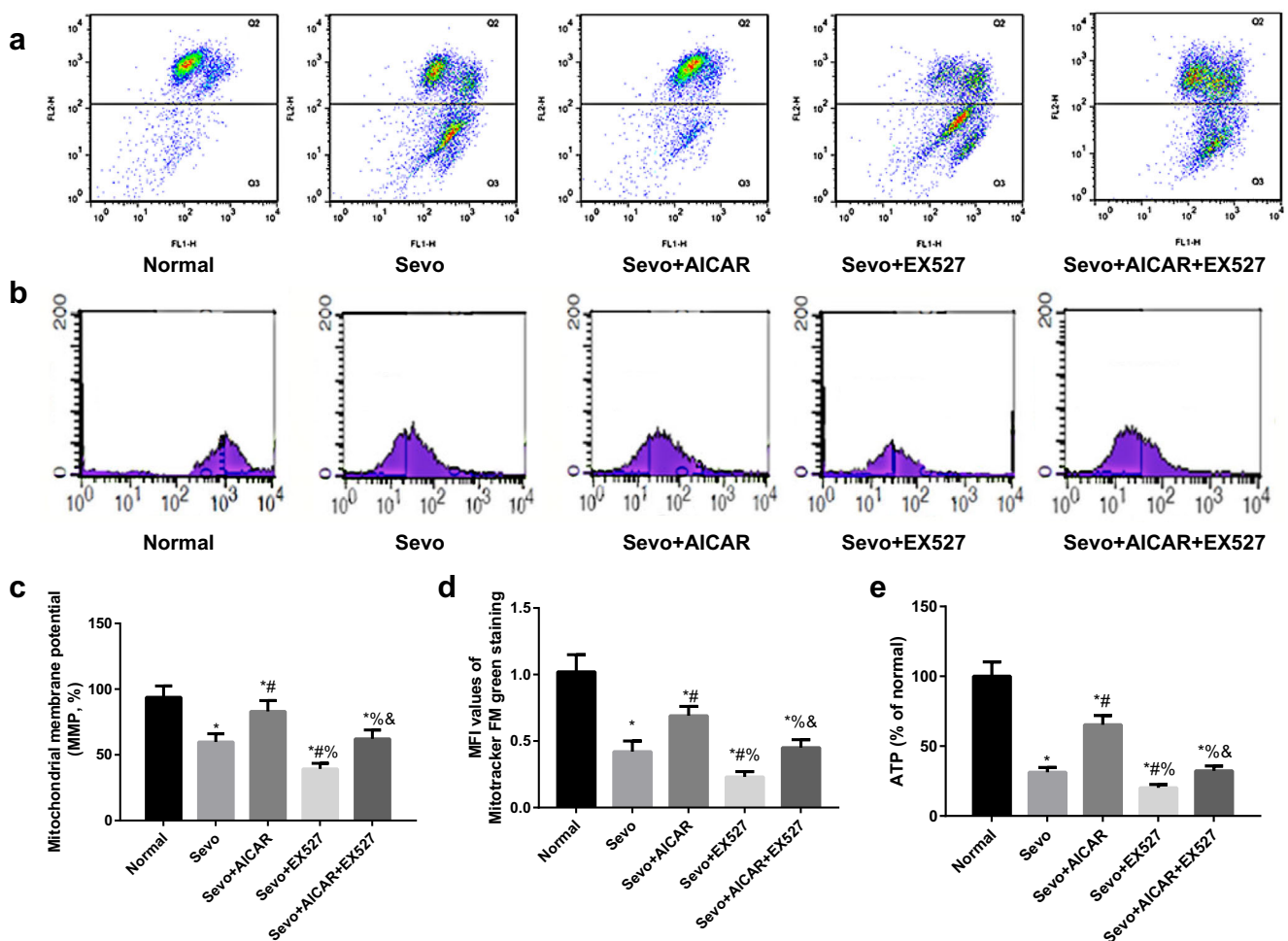
Fig. 4 Comparison of levels of MMP and ATP of rats among groups. **a** Variations in MMP determined by JC-1 probe in flow cytometer; **b** fluorescence-activated cell sorting (FACS) results for MitoTracker Green FM staining; **c** comparison of the MMP levels of rats among groups; **d** the mean fluorescence intensity (MFI) values of MitoTracker Green FM staining relative to Normal group are shown; **e** Comparison of

the ATP levels of rats among groups; the data are expressed as mean ± SD (one-way ANOVA followed by Turkey's post hoc test, $n = 12$). * $P < 0.05$ vs. the Normal group; # $P < 0.05$ vs. the Sevo group; % $P < 0.05$ vs. the Sevo + AICAR group; & $P < 0.05$ vs. the Sevo + EX527 group

expression of PGC1α (Nemoto et al. 2005). Therefore, the activation of AMPK-SIRT1-PGC-1α in our models may improve the learning and memory abilities of sevoflurane-anesthetized elder rats.

Hippocampal oxidative injury, as one of the pathological hallmarks in sevoflurane-induced POCD, is also detected in our study by measuring the MDA level and SOD activity (Yang et al. 2014). As a result, sevoflurane anesthesia increases the MDA level and ROS generation but declines the activity of SOD, which, however, is reversed by AMPK activation, but deteriorated by EX527 treatment. Furthermore, neuronal apoptosis is confirmed as one of the mechanisms in sevoflurane-induced neuronal toxicity (Dong et al. 2009), whereas mitochondrion is the major place for modulation of cell apoptosis and generation of free radicals, where the accumulating free radicals can peroxidase the lipid on the mitochondrial membrane to activate the mitochondrial apoptosis

pathway, eventually inducing cell apoptosis or necrosis (Naoi et al. 2005; Radi et al. 2014). More importantly, mitochondrial membrane potential (MMP) is the major indicator reflecting the integrity of mitochondrial function (Iijima 2006), while the neuronal function depends on the energy released from the oxidation or phosphorylation of ATP in mitochondrion (Alves et al. 2017). In the hippocampus of our sevoflurane-anesthetized rats, the apoptotic and degenerating neurons are increased, with up-regulation of cleaved caspase-3 and decreases in MMP and ATP, which is fully reversed by the activation of AMPK-SIRT1-PGC-1α. Besides, MitoTracker Green FM staining was used for the determination of relative mitochondrial mass in individual cells (Conca Dioguardi et al. 2016), and we found that the activation of AMPK also elevated the mitochondrial mass, possibly due to the enhanced mitochondrial activity according to a previous study (Shimura et al. 2017). Consistent with our findings, Yao et al. (2019)
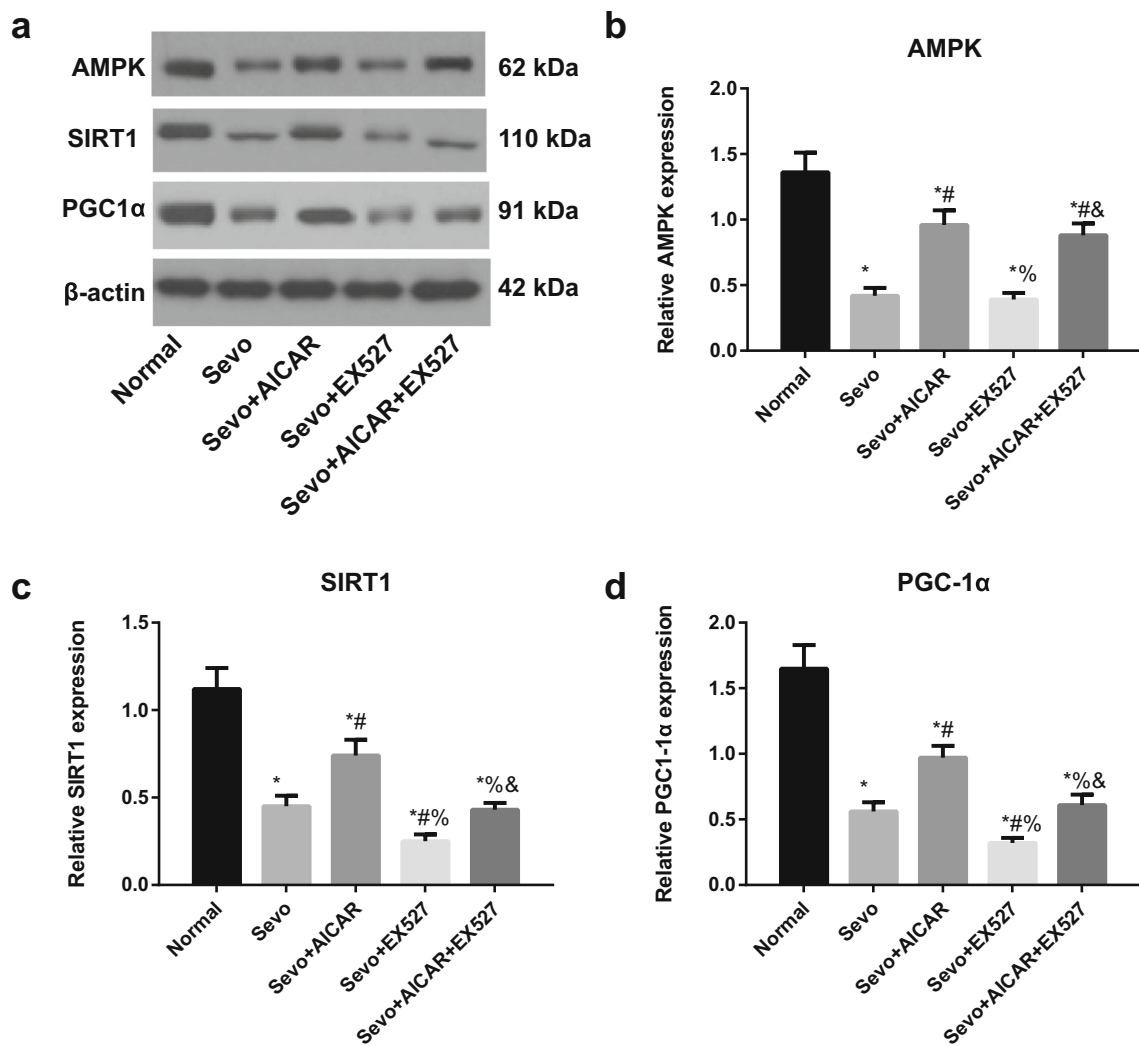
Fig. 5 Expression of AMPK-SIRT1-PGC-1α signaling pathway. **a** Protein expressions in AMPK-SIRT1-PGC-1αpathway detected by Western blotting; **b–d** Comparison of the expressions of AMPK, SIRT1, and PGC-1α in hippocampus of rats among groups; the data are presented as the mean ± SD (one-way ANOVA followed by Turkey's post hoc test, $n = 12$). * $P < 0.05$ vs. the Normal group; # $P < 0.05$ vs. the Sevo group; % $P < 0.05$ vs. the Sevo + AICAR group; & $P < 0.05$ vs. the Sevo + EX527 group

found the improved cognitive dysfunction owing to the activation of SIRT1/PGC-1α pathway to inhibit neuronal apoptosis and play antioxidant effects. Yu et al. (2018) also noted that berberine can increase the generation of ATP and reduce the level of ROS in skeletal muscle via activating AMPK/SIRT1/PGC-1α pathway, thereby improving the cognitive dysfunction in naturally aged rats. In STZ-induced Alzheimer's disease rats, Du et al. (2015) also discovered that AICAR-activated AMPK can increase the level of ATP, MMP, and activity of complex I, thus ameliorating the mitochondrial function and the cognitive function of rats. Existing evidence has confirmed that AMPK activation can increase the activity of SIRT1, and the interaction between them can trigger the biological development of mitochondrion and regulate the activity of PGC-1α, whereas PGC-1α, by binding PPARγ, can modulate the proteins that are critical to the regulation of biological synthesis of mitochondrion and promote the replication of genes that are associated with the oxidative phosphorylation of mitochondria and mitochondrial DNA, thereby modulating the mitochondrial function and metabolism positively (Jimenez-Flores et al. 2014; Park et al. 2012; Zu et al. 2010). Taken together, activation of AMPK-SIRT1-PGC-1α signal pathway can ameliorate the learning and memory ability in sevoflurane-anesthetized rats, which may attribute to the mitigation of oxidative stress and mitochondrial activation that can antagonize the sevoflurane-induced neuronal apoptosis and enhance the generation of ATP. We also examined the level of GFAP, a marker of activated astrocytes, since astrocyte function may affect the cognition and memory (Jin et al. 2014).Then, we observed that the activation of AMPK down-regulated the fluorescence intensity of GFAP in sevoflurane-induced rats, suggesting that AMPK activation may reduce the impairment of neurobehavioral functions by inhibiting the activation of astrocytes.

There were some limitations to the present study. Firstly, the technique in terms of invasivity and high cost in our study prevents from using this experimental evidence in the clinical practice. Secondly, only animal experiments were carried out in this study, as there are some approved drugs for activating the AMPK; a clinical trial would be an important next step in our future studies to validate the experimental results that activation of AMPK-SIRT1-PGC-1α pathway can improve the cognitive function and mitigate the neuronal injury in sevoflurane-anesthetized aged rats.

In conclusion, activation of AMPK-SIRT1-PGC-1α pathway can antagonize the oxidative stress and sustain the mitochondrial function to improve the cognitive function and mitigate the neuronal injury in sevoflurane-anesthetized aged rats, which can serve as the novel theoretical evidence for treatment of sevoflurane-induced POCD.

Compliance with Ethical Standards

Competing Interests The authors declare that they have no competing interests.

References

Alves M et al (2017) Expression and function of the metabotropic purinergic P2Y receptor family in experimental seizure models and patients with drug-refractory epilepsy. Epilepsia 58:1603–1614. https://doi.org/10.1111/epi.13850

Austin S, St-Pierre J (2012) PGC1alpha and mitochondrial metabolism–emerging concepts and relevance in ageing and neurodegenerative disorders. J Cell Sci 125:4963–4971. https://doi.org/10.1242/jcs.113662

Canto C, Auwerx J (2009) PGC-1alpha, SIRT1 and AMPK, an energy sensing network that controls energy expenditure. Curr Opin Lipidol 20:98–105. https://doi.org/10.1097/MOL.0b013e328328d0a4

Cao K et al (2014) AMPK activation prevents prenatal stress-induced cognitive impairment: modulation of mitochondrial content and oxidative stress free. Radic Biol Med 75:156–166. https://doi.org/10.1016/j.freeradbiomed.2014.07.029

Chau MD, Gao J, Yang Q, Wu Z, Gromada J (2010) Fibroblast growth factor 21 regulates energy metabolism by activating the AMPK-SIRT1-PGC-1alpha pathway. Proc Natl Acad Sci U S A 107:12553–12558. https://doi.org/10.1073/pnas.1006962107

Chung S, Yao H, Caito S, Hwang JW, Arunachalam G, Rahman I (2010) Regulation of SIRT1 in cellular functions: role of polyphenols arch. Biochem Biophys 501:79–90. https://doi.org/10.1016/j.abb.2010.05.003

Claret M et al (2007) AMPK is essential for energy homeostasis regulation and glucose sensing by POMC and AgRP neurons. J Clin Invest 117:2325–2336. https://doi.org/10.1172/JCI31516

Conca Dioguardi C et al (2016) Granulosa cell and oocyte mitochondrial abnormalities in a mouse model of fragile X primary ovarian insufficiency. Mol Hum Reprod 22:384–396. https://doi.org/10.1093/molehr/gaw023

Cremer J, Stoppe C, Fahlenkamp AV, Schalte G, Rex S, Rossaint R, Coburn M (2011) Early cognitive function, recovery and well-being after sevoflurane and xenon anaesthesia in the elderly: a double-blinded randomized controlled trial. Med Gas Res 1:9. https://doi.org/10.1186/2045-9912-1-9

Davis N, Lee M, Lin AY, Lynch L, Monteleone M, Falzon L, Ispahany N, Lei S (2014) Postoperative cognitive function following general versus regional anesthesia: a systematic review. J Neurosurg Anesthesiol 26:369–376. https://doi.org/10.1097/ANA.0000000000000120

Delgado-Herrera L, Ostroff RD, Rogers SA (2001) Sevoflurance: approaching the ideal inhalational anesthetic. A pharmacologic, pharmacoeconomic, and clinical review. CNS Drug Rev 7:48–120. https://doi.org/10.1111/j.1527-3458.2001.tb00190.x

Dong Y et al (2009) The common inhalational anesthetic sevoflurane induces apoptosis and increases beta-amyloid protein levels. Arch Neurol 66:620–631. https://doi.org/10.1001/archneurol.2009.48

Dong W, Wang F, Guo W, Zheng X, Chen Y, Zhang W, Shi H (2016) Abeta25-35 suppresses mitochondrial biogenesis in primary hippocampal neurons. Cell Mol Neurobiol 36:83–91. https://doi.org/10.1007/s10571-015-0222-6

Du LL et al (2015) AMPK activation ameliorates Alzheimer's disease-like pathology and spatial memory impairment in a streptozotocin-induced Alzheimer's disease model in rats. J Alzheimers Dis 43:775–784. https://doi.org/10.3233/JAD-140564

Gong M, Chen G, Zhang XM, Xu LH, Wang HM, Yan M (2012) Parecoxib mitigates spatial memory impairment induced by sevoflurane anesthesia in aged rats. Acta Anaesthesiol Scand 56:601–607. https://doi.org/10.1111/j.1399-6576.2012.02665.x

Haseneder R, Kratzer S, von Meyer L, Eder M, Kochs E, Rammes G (2009) Isoflurane and sevoflurane dose-dependently impair hippocampal long-term potentiation. Eur J Pharmacol 623:47–51. https://doi.org/10.1016/j.ejphar.2009.09.022

Hu N et al (2014) Involvement of the blood-brain barrier opening in cognitive decline in aged rats following orthopedic surgery and high concentration of sevoflurane inhalation. Brain Res 1551:13–24. https://doi.org/10.1016/j.brainres.2014.01.015

Hwang JW, Yao H, Caito S, Sundar IK, Rahman I (2013) Redox regulation of SIRT1 in inflammation and cellular senescence free. Radic Biol Med 61:95–110. https://doi.org/10.1016/j.freeradbiomed.2013.03.015

Iijima T (2006) Mitochondrial membrane potential and ischemic neuronal death. Neurosci Res 55:234–243. https://doi.org/10.1016/j.neures.2006.04.005

Jimenez-Flores LM, Lopez-Briones S, Macias-Cervantes MH, Ramirez-Emiliano J, Perez-Vazquez V (2014) A PPARgamma, NF-kappaB and AMPK-dependent mechanism may be involved in the beneficial effects of curcumin in the diabetic db/db mice liver. Molecules 19:8289–8302. https://doi.org/10.3390/molecules19068289

Jin WJ, Feng SW, Feng Z, Lu SM, Qi T, Qian YN (2014) Minocycline improves postoperative cognitive impairment in aged mice by inhibiting astrocytic activation. Neuroreport 25:1–6. https://doi.org/10.1097/WNR.0000000000000082

Jungwirth B, Zieglgansberger W, Kochs E, Rammes G (2009) Anesthesia and postoperative cognitive dysfunction (POCD). Mini Rev Med Chem 9:1568–1579. https://doi.org/10.2174/138955709791012229

Kim D et al (2007) SIRT1 deacetylase protects against neurodegeneration in models for Alzheimer's disease and amyotrophic lateral sclerosis. EMBO J 26:3169–3179. https://doi.org/10.1038/sj.emboj.7601758

Li J, Zhou J, Wan Y, Liu L, Ou C (2017) Association between ABO blood type and postoperative cognitive dysfunction in elderly patients undergoing unilateral total hip arthroplasty surgery in China. Med Sci Monit 23:2584–2589. https://doi.org/10.12659/msm.901736

Liu C, Han JG (2015) Advances in the mechanisms and early warning indicators of the postoperative cognitive dysfunction after the extracorporeal circulation. Zhongguo Yi Xue Ke Xue Yuan Xue Bao 37:101–107. https://doi.org/10.3881/j.issn.1000-503X.2015.01.019

Liu X, Song X, Yuan T, He J, Wang X, Wang Q (2016) Effects of calpain on sevoflurane-induced aged rats hippocampal neuronal apoptosis. Aging Clin Exp Res 28:633–639. https://doi.org/10.1007/s40520-015-0466-5

Lu J et al (2010) Quercetin activates AMP-activated protein kinase by reducing PP2C expression protecting old mouse brain against high cholesterol-induced neurotoxicity. J Pathol 222:199–212. https://doi.org/10.1002/path.2754

Mason TJ, Matthews M (2012) Aquatic environment, housing, and management in the eighth edition of the guide for the care and use of laboratory animals: additional considerations and recommendations. J Am Assoc Lab Anim Sci 51:329–332

Naoi M, Maruyama W, Shamoto-Nagai M, Yi H, Akao Y, Tanaka M (2005) Oxidative stress in mitochondria: decision to survival and death of neurons in neurodegenerative disorders. Mol Neurobiol 31:81–93. https://doi.org/10.1385/MN:31:1-3:081

Nemoto S, Fergusson MM, Finkel T (2005) SIRT1 functionally interacts with the metabolic regulator and transcriptional coactivator PGC-1{alpha}. J Biol Chem 280:16456–16460. https://doi.org/10.1074/jbc.M501485200

Nesaratnam A, Nesaratnam N, Agius M (2014) Cognitive impairment following use of anaesthetic agents: a review of the literature, and implications for future practice. Psychiatr Danub 26(Suppl 1):53–55

Ning H, Cao D, Wang H, Kang B, Xie S, Meng Y (2017) Effects of haloperidol, olanzapine, ziprasidone, and PHA-543613 on spatial learning and memory in the Morris water maze test in naive and MK-801-treated mice. Brain Behav 7:e00764. https://doi.org/10.1002/brb3.764

Park SJ et al (2012) Resveratrol ameliorates aging-related metabolic phenotypes by inhibiting cAMP phosphodiesterases. Cell 148:421–433. https://doi.org/10.1016/j.cell.2012.01.017

Radi E, Formichi P, Battisti C, Federico A (2014) Apoptosis and oxidative stress in neurodegenerative diseases. J Alzheimers Dis 42(Suppl 3):S125–S152. https://doi.org/10.3233/JAD-132738

Shimura T, Sasatani M, Kawai H, Kamiya K, Kobayashi J, Komatsu K, Kunugita N (2017) A comparison of radiation-induced mitochondrial damage between neural progenitor stem cells and differentiated cells. Cell Cycle 16:565–573

Steinmetz J, Christensen KB, Lund T, Lohse N, Rasmussen LS, Group I (2009) Long-term consequences of postoperative cognitive dysfunction. Anesthesiology 110:548–555. https://doi.org/10.1097/ALN.0b013e318195b569

Tian Y, Guo S, Wu X, Ma L, Zhao X (2015) Minocycline alleviates sevoflurane-induced cognitive impairment in aged rats. Cell Mol Neurobiol 35:585–594. https://doi.org/10.1007/s10571-014-0154-6

Xie J, Zhang X, Zhang L (2013) Negative regulation of inflammation by SIRT1. Pharmacol Res 67:60–67. https://doi.org/10.1016/j.phrs.2012.10.010

Yan W, Fang Z, Yang Q, Dong H, Lu Y, Lei C, Xiong L (2013) SirT1 mediates hyperbaric oxygen preconditioning-induced ischemic tolerance in rat brain. J Cereb Blood Flow Metab 33:396–406. https://doi.org/10.1038/jcbfm.2012.179

Yan WJ, Wang DB, Ren DQ, Wang LK, Hu ZY, Ma YB, Huang JW, Ding SL (2019) AMPKalpha1 overexpression improves postoperative cognitive dysfunction in aged rats through AMPK-Sirt1 and autophagy signaling. J Cell Biochem 120:11633–11641. https://doi.org/10.1002/jcb.28443

Yang C, Zhu B, Ding J, Wang ZG (2014) Isoflurane anesthesia aggravates cognitive impairment in streptozotocin-induced diabetic rats. Int J Clin Exp Med 7:903–910

Yao P, Li Y, Yang Y, Yu S, Chen Y (2019) Triptolide improves cognitive dysfunction in rats with vascular dementia by activating the SIRT1/PGC-1alpha signaling pathway. Neurochem Res 44:1977–1985. https://doi.org/10.1007/s11064-019-02831-3

Yu Y et al (2018) Berberine improves cognitive deficiency and muscular dysfunction via activation of the AMPK/SIRT1/PGC-1a pathway in skeletal muscle from naturally aging rats. J Nutr Health Aging 22:710–717. https://doi.org/10.1007/s12603-018-1015-7

Zhang L, Zhang J, Yang L, Dong Y, Zhang Y, Xie Z (2013) Isoflurane and sevoflurane increase interleukin-6 levels through the nuclear factor-kappa B pathway in neuroglioma cells. Br J Anaesth 110(Suppl 1):i82–i91. https://doi.org/10.1093/bja/aet115

Zhao Z, Yao M, Wei L, Ge S (2019) Obesity caused by a high-fat diet regulates the Sirt1/PGC-1alpha/FNDC5/BDNF pathway to exacerbate isoflurane-induced postoperative cognitive dysfunction in older mice. Nutr Neurosci:1–12. https://doi.org/10.1080/1028415X.2019.1581460

Zu Y et al (2010) SIRT1 promotes proliferation and prevents senescence through targeting LKB1 in primary porcine aortic endothelial cells. Circ Res 106:1384–1393. https://doi.org/10.1161/CIRCRESAHA.109.215483